Available online at www.sciencedirect.com
ScienceDirect
Journal of Fluorine Chemistry 128 (2007) 1359–1368
JOURNAL OF FLUORINE CHEMISTRY
www.elsevier.com/locate/fluor

Surface and bulk properties of severely fluorinated carbon fibres

Kingsley K.C. Ho [a], Graham Beamson [b], George Shia [c], Natalya V. Polyakova [d], Alexander Bismarck [a,*]

[a] *Department of Chemical Engineering, Polymer and Composite Engineering (PaCE) Group, Imperial College London, London SW7 2AZ, UK*
[b] *STFC Daresbury Laboratory, National Centre for Electron Spectroscopy and Surface Analysis, Daresbury, Warrington, Cheshire WA4 4AD, UK*
[c] *Lodestar Ltd. Inc., 8 Arbor Drive, Howell, NJ 07731, USA*
[d] *SRI "Electrical Carbon Products" Electrougly, Moscow 142455, Russia*

Received 20 April 2007; received in revised form 5 June 2007; accepted 14 June 2007
Available online 19 June 2007

Abstract

The development of ultra-inert composites using fluorinated carbon fibres as the reinforcement requires fluorinated carbon fibres with a durable surface composition. Here we report the effect of direct fluorination using an F_2/N_2 mixture at 653 K on the surface and bulk properties of two types of high strength carbon fibres. These were treated up to a surface fluorine content of ~64 at.% and a bulk fluorine content of ~15 mass%. A colour change was observed after fluorination caused by the changes in the graphitic band structure of the carbon fibres by the introduction of carbon sp^3 hybridisation. The tensile strength and Young's modulus decrease after fluorination by up to 33 and 22%, respectively. XRD shows marginal changes in the interlayer distance but the crystallite size increases. Changes in the electrical conductivity of the fluorinated carbon fibres indicate that the modification is confined to the near surface volume. Predominantly covalent C–F bonds are formed as shown by X-ray photoelectron spectroscopy (XPS) and measured zeta (ζ)-potentials. Hence the fluorinated fibres are hydrophobic and have low surface tensions. This and the large increase in fibre surface area, as determined by nitrogen adsorption, is expected to facilitate interfacial interaction between fluorinated carbon fibres and fluoropolymers.

Keywords: Carbon fibres; Direct fluorination; Surface and bulk properties; Zeta potential; Contact angle; XPS

1. Introduction

Ever since carbon fibres were first produced in the early 1960s they have remained amongst the most commonly used high performance reinforcing fibres for the manufacture of composite materials. They offer not only exceptional mechanical strength but also chemical stability. The fibre chemistry can be adjusted by various means to bond to a desired matrix material [1]. Fibre reinforced composite materials have been first choice materials for aerospace, automobile and sporting goods, etc. because of their high strength, high modulus and low density [2,3].

Fluoropolymers exhibit excellent toughness and corrosion resistance to severe environmental stresses [4,5]. They offer great potential as a matrix for fibre reinforced composites for applications in harsh environments such as those encountered in the oil, gas and chemical industries [6,7]. Fluoropolymers are however extremely hydrophobic and their adhesion to reinforcing fibres is poor [8]. There is increasing evidence that the fluorination of carbon fibres leads to a much-improved interaction between such fibres and fluoropolymers [9–11]. Carbon fibres can be fluorinated directly [12] or using low pressure [13,14] and even atmospheric pressure plasmas [15]. Direct fluorination of carbon fibres was investigated by Gupta et al. and Tressaud et al. [16–18]. They found that the thermal stability of fluorine-intercalated carbon fibres depends on the different types of C–F bonds formed. This in turn is linked to the physico-chemical characteristics of the pristine carbon fibres, whether they are polyacrylonitrile (PAN) or pitch-based, and to the experimental conditions of the fluorination procedure. The bonding between F and C can range from covalent through semi-ionic to ionic [12]. The hydrophobicity [12] of fluorinated carbon fibres and their reduced electrical conductivity is due to the formation of covalent C–F bonds during the fluorination process [14]. The colour changes which

* Corresponding author. Tel.: +44 207594 5578; fax: +44 207594 5638.
E-mail address: a.bismarck@imperial.ac.uk (A. Bismarck).

0022-1139/$ – see front matter © 2007 Elsevier B.V. All rights reserved.
doi:10.1016/j.jfluchem.2007.06.005

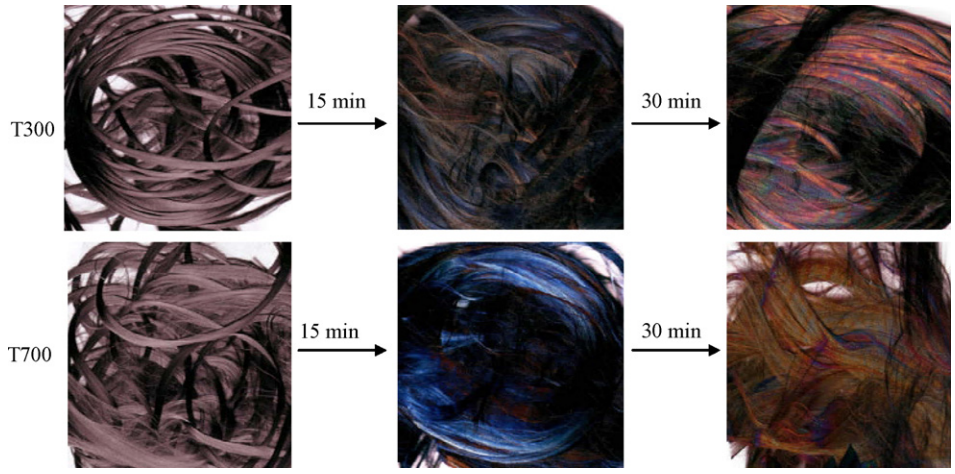

Fig. 1. Scanned images of the colour of fluorinated T300 and T700SC carbon fibres with increasing fluorination time.

take place during fluorination of carbon fibres are due to the formation of intercalated fluorine species [19].

For composite applications, durable long lasting surface modifications are required. If the fibre surface composition and hence the fibre/matrix interface changes with time, for example by ion exchange or leakage of ionically bound fluorine from the fibres, the mechanical properties of the composite will also be affected. As a result, we are interested in scalable procedures that allow a wide range of degrees of fluorination of carbon fibres and enable the adhesion to the fluoropolymer matrix to be tailored for effective load transfer from matrix to fibres. In this study, we report the use of F_2/N_2 mixtures to fluorinate carbon fibres and the effect of this direct fluorination procedure on the resulting surface and bulk properties of the fibres.

2. Results and discussion

2.1. Appearance of directly fluorinated carbon fibres

The observed colour change of the carbon fibres after direct fluorination is supposedly a good indication of bulk fluorination (Fig. 1 provides a selected subset of scanned images. The complete set of images can be found as Supplementary Figs. 1 and 2 online), which signifies different intercalation stages [20], however this phenomenon was not observed, which will be discussed later. Reaction between fluorine and graphitic materials is known to result in a variety of different types of compounds, such as a change from sp^2 state of the graphitic layers to the sp^3 state. This leads to colour changes and eventually the material becomes colourless [21]. As fluorination time increases the carbon fibres change colour from matt black through violet to brown while maintaining a surface F/C ratio of around 1.7. This shows that the increasing exposure time to fluorine atmosphere changes the carbon fibres structure and electronic properties to a certain extent but not as vigorous compared to the work of Touhara et al. [19].

2.2. Bulk and surface fluorine concentration

Table 1 shows the bulk fluorine content of the fluorinated carbon fibres, as determined by chemical analysis. A steady increase of the bulk fluorine content with fluorination time up to

Table 1
Surface and bulk fluorine content of direct fluorinated FT 300 and T700SC carbon fibres

Fibre	Fluorination Duration (min)	Fibre Abbreviation		Bulk F Content / mass %	Surface F Content %				
					C / at.-%	F / at.-%	O / at.-%	N / at.-%	O:C
T300	0		T3A	-	88.7	-	11.3	-	0.13
	15		T3B	6.50	35.5	64.5	-	-	0
	20	T3*	T3C	8.30	37.4	60.7	0.6	1.2	0.02
	25		T3D	10.0	36.4	63.6	-	-	0
	30		T3E	14.4	36.9	61.5	0.4	1.1	0.01
T700	0		T7A	-	82.1	-	2.5	14.1	0.03
	15		T7B	4.7	34.3	64.8	0.9	-	0
	20	T7*	T7C	6.8	39.2	59.1	0.6	1	0.02
	25		T7D	8.7	34.8	64.1	0.4	0.7	0.01
	30		T7E	10.4	33.5	65.4	0.4	0.7	0.01

Table 2
C 1s, F 1s and O 1s binding energies, relative amounts and C/F ratios of direct fluorinated T300 and T700SC carbon fibres

	Assignment	T3A	T3B	T3C	T3D	T3E	T7A	T7B	T7C	T7D	T7E
C 1s	Graphite C	284.5	285.5	288.4	286.1	288.0	284.6	289.6	285.3	285.9	285.1
		48.1	10.9	5.6	3.7	2.4	42.3	5.6	3.9	4.9	3.5
	C–O	285.9					285.4				
		44.1					38.8				
	C═O	289.3					288.2		287.8		287.8
		7.9					18.0		1.3		2.6
	CF		290.2	290.4	290.3	290.3		290.5	290.3	290.6	290.3
			18.1	57.7	44.9	53.3		38.5	53.8	41.0	46.2
	CF_2		291.2	292.0	291.4	291.7		291.1	291.9	292.1	291.7
			53.1	31.8	24.3	33.2		34.9	34.5	49.3	41.6
	CF_3		294.4	294.2	291.8	293.4		293.1	293.9	292.1	294.1
			17.9	4.8	27.1	11.1		21.0	6.5	4.8	6.2
F 1s	Covalent F–C		689.0	689.2	689.2	690.2		689.7	689.3	689.6	689.3
O 1s		533.0	535.7	536.0	535.9	536.1	531.0	536.4	536.0	527.3	535.8
F/C ratio			1.87	1.62	1.75	1.67		1.67	1.89	1.84	1.95

14.4 mass% for the T300 fibres (T3A–T3E) and 10.4 mass% for the T700 fibres (T7A–T7E) at 30 min was observed. The reaction between fluorine and the carbon fibres consists of two simultaneous but competing processes: (1) the desired formation of solid fluorinated carbon and (2) a combustion reaction leading to the formation of gaseous fluorides, e.g. CF_4 and C_2F_6 and, therefore, to the removal of carbon from the fibres. The second process is the primary cause for the morphological inhomogeneities in the fibre surfaces and will be discussed in more detail later.

The influence of the fluorination time on the surface composition of the fibres was investigated by XPS (Table 1). The industrially electrochemically oxidised and desized T3A and T7A fibres are fluorine-free, but contain significant amounts of oxygen. Direct fluorination results in a dramatic change in the overall surface composition—the introduction of F and a reduction in the at.% of C. The surface fluorine content is almost independent of the fluorination time and of the substrate used.[1] For the T300 series the surface fluorine concentration is constant at 62.6 ± 0.8 at.% and for the T700 series at 63.4 ± 1.4 at.%. A measure of the changes in surface polarity/hydrophobicity can also be garnered by examining the evolution of the O:C ratio across the series. This decreases from 0.1 to 0.01 following the longest fluorination treatment of the T300 series and from 0.03 to 0.01 for the T700 series. In some cases complete removal of oxygen functionalities was also observed (Table 1).

These compositional changes are reflected in the corresponding high resolution C 1s XP spectra scans (Table 2) with a remarkable change between the non-fluorinated (T3A, T7A) and fluorinated fibres (T3B–T3E, T7B–T7E). The graphitic/aliphatic carbon environment at 285 eV binding energy is not present after fluorination and instead states at 290, 292 and 294 eV are observed. These correspond to carbon in: C–F, CF_2 and CF_3 chemical environments [22]. The C–O and C═O peaks are not detected after fluorination except for the T7C and T7E fibres where a small trace of C═O is still present on the fibre surface. The high resolution F 1s XP spectra of the fluorinated T300 and T700 carbon fibres show a single component at ~689.0 eV for all fluorination times (Table 2), indicating that the fluorine is covalently bound to the carbon surface [12].

2.3. Surface properties of directly fluorinated fibres

2.3.1. Wettability and surface tension of severely fluorinated carbon fibres

The wetting behaviour of the fluorinated fibres was investigated using the modified Wilhelmy technique [23]. The fibre surfaces become significantly more hydrophobic, as a result of direct fluorination, as shown by the dramatic increase of the advancing water contact angle θ_a from 79° to 115° (T3A–T3E) and from 73° to 103° (T7A–T7E) (Table 3). This sharp rise in the surface hydrophobicity is due to the increase in the F:C ratio and the absence of hydrophilic ionic C–F bonds. For the T300 series the receding water contact angle θ_r remains constant within the experimental error. The receding contact angle θ_r measured during the de-wetting process, is more characteristic of the high-energy component of the wetted surface. Once established, the attractive interaction between water and the few remaining polar functional groups has to be overcome. The water contact angle hysteresis $\Delta\theta$ defined as the difference between θ_a and the θ_r, increases for the fluorinated T300 and T700 carbon fibres. For diiodomethane (DIM), i.e. a purely non-polar test liquid, θ_a increases dramatically on fluorination which reflects the change in the nature of the carbon fibre surface from a (turbostratic) graphitic surface to a fully fluorinated surface. For DIM $\Delta\theta$ also increases after direct fluorination. The occurrence of contact angle hysteresis is due to chemical heterogeneities and/or surface roughness [24,25].

[1] Direct fluorination on Hexcel IM7 (HS-CP-5000) carbon fibres was also performed, for which the bulk F content increases to 11.2 mass% and the surface F content remains at 65 at.%.

Table 3
Surface-free energies (γ_s^{EoS}) and dynamic contact angles of direct fluorinated T300 and T700SC carbon fibres against water (W), diiodomethane (DIM) and formamide (FA)

Fibre	d_f (μm)	θ_a (W) (°)	θ_r (W) (°)	θ_a (DIM) (°)	θ_r (DIM) (°)	θ_a (FA) (°)	θ_r (FA) (°)	γ_θ^{EOS} (mN m^{-1})
T3A	7.0 ± 0.3	79.2 ± 1.4	61.7 ± 1.2	60.5 ± 1.56	58.0 ± 1.1	65.4 ± 0.7	61.6 ± 1.5	44.0 ± 3.9
T3B	7.3 ± 0.2	116.1 ± 2.3	64.7 ± 6.5	82.8 ± 2.6	44.8 ± 2.8	91.7 ± 1.5	35.5 ± 1.7	21.3 ± 3.1
T3C	7.0 ± 0.1	95.2 ± 6.2	65.4 ± 2.2	78.7 ± 4.3	44.8 ± 1.4	91.6 ± 1.8	24.5 ± 3.4	23.6 ± 0.2
T3D	7.2 ± 0.2	106.8 ± 3.8	69.6 ± 4.0	82.5 ± 2.3	46.6 ± 1.0	93.4 ± 3.2	30.2 ± 6.2	21.9 ± 2.3
T3E	7.3 ± 0.1	116.5 ± 1.1	60.1 ± 6.9	87.7 ± 0.5	46.9 ± 4.1	88.6 ± 2.9	52.3 ± 1.2	20.3 ± 2.5
T7A	6.3 ± 0.6	72.9 ± 2.7	43.6 ± 4.8	30.5 ± 5.1	11.4 ± 5.5	38.0 ± 2.4	28.0 ± 1.6	31.4 ± 1.8
T7B	6.9 ± 0.2	108.6 ± 3.7	57.9 ± 1.8	79.6 ± 1.37	51.2 ± 1.8	83.6 ± 1.9	38.6 ± 3.5	17.9 ± 3.7
T7C	7.2 ± 0.1	99.3 ± 4.3	60.1 ± 5.7	75.4 ± 4.2	57.9 ± 5.1	84.8 ± 0.5	33.2 ± 1.2	22.7 ± 3.1
T7D	7.1 ± 0.1	97.7 ± 2.2	72.8 ± 5.3	80.7 ± 1.8	53.7 ± 0.9	91.5 ± 4.3	26.4 ± 4.2	19.4 ± 0.8
T7E	6.8 ± 0.5	102.6 ± 4.5	70.3 ± 5.7	79.1 ± 2.1	43.3 ± 4.2	96.2 ± 2.3	18.8 ± 4.0	17.6 ± 4.0

From the contact angles measured between the fluorinated fibres, water, formamide and DIM, the surface tension γ_s of direct fluorinated carbon fibres was calculated using the Neumann's equation-of-state method [26] (Table 3). The surface tension decreases from values over 30 to 19.4 ± 1.2 mN m^{-1} for T300 and to 21.8 ± 0.7 mN m^{-1} for T700 carbon fibres after fluorination due to the incorporation of fluorine moieties into the fibre surfaces. This is expected with the increase in surface hydrophobicity post fluorination caused by the presence of covalent C–F$_x$ bonds. The surfaces of the fluorinated carbon fibres indeed became PTFE-like which has a surface tension of 18.5 mN m^{-1} [27].

2.3.2. Surface area of direct fluorinated carbon fibres

During direct fluorination, carbon material is converted into gaseous fluorocarbons but nevertheless for the T300 fibres the fibre diameter remains constant. For the T700 fibres it even increases slightly as the bulk fluorine content increases. An increase in the fibre surface area and the removal of weakly attached surface layers can enhance the measured practical adhesion between modified fibres and the matrix in carbon fibre composites [28]. Therefore, we investigated the influence of direct fluorination on the surface area of the carbon fibres. The original desized but industrially oxidised T300 and T700 carbon fibres have a BET surface area of 0.47 and 0.22 m^2 g^{-1} prior to the exposure to fluorine. The BET surface area of the T300 fibres increased steadily with increasing fluorination time up to 38.1 m^2 g^{-1} (Fig. 2) and that of the T700 fibres increased to 33.4 m^2 g^{-1} after 30 min fluorination.

SEM micrographs (Fig. 3 provides a selected subset of SEM images. The complete set of images can be found as Supplementary Figs. 3 and 4 online) show that T300 fibres have the typical surface appearance of PAN-based carbon fibres with striations along the fibre axis. In contrast the desized but industrially oxidised T700 fibres have no apparent striations. After 30 min exposure to the fluorination atmosphere a significant surface damage of the fibres was observed (Fig. 3), which explains the sharp increase in BET surface area. However, rather surprisingly the observed contact angle hysteresis for all three test liquids used, remains largely unaffected by the increasing exposure time to fluorine and, therefore, the increase in fibre surface area. This leads to the conclusion that the increase in contact angle hysteresis has to be solely due to the presence of the few remaining polar groups on the carbon fibre surfaces after direct fluorination, affecting the de-wetting behaviour.

2.3.3. Surface character: ζ-potentials

The ζ-potentials of the fluorinated fibres were obtained from measured streaming potentials. Measurements of the ζ-potential as a function of time enable identification of the different kinds of chemical bonds between fluorine and carbon materials [29]. As exemplarily shown in Fig. 4a, the electrical conductivity of the supporting KCl electrolyte increased only slightly while the pH remained constant over a period of 1600 min. XPS indicated the presence of only covalent CF bonds but the small increase in conductivity could be due to the presence of a low concentration of ionic character C–F bonds, which dissociate in contact with water. The ζ-potentials increase with time from a negative starting value and approach an equilibrium value asymptotically. The ζ-potential stabilises within 120 min for most of the fluorinated T300 fibres (Fig. 4b) and within 600 min (Fig. 4c) for the fluorinated T700 carbon fibres. The time-dependence of the ζ-potentials reflects the time it takes for the few ionic character C–F bonds (including those from the bulk) to dissociate in water.

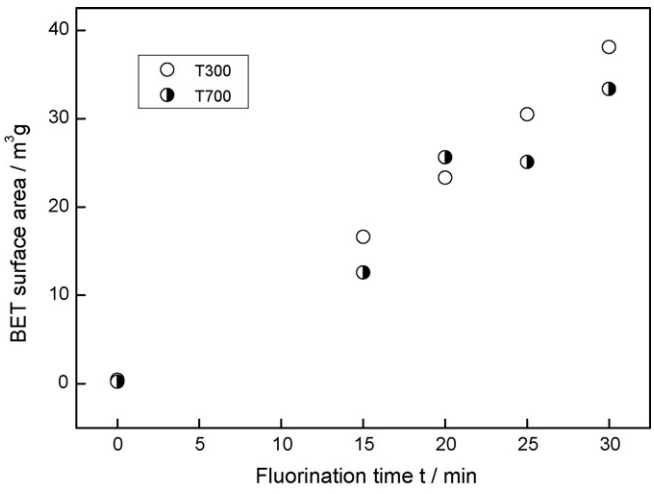

Fig. 2. BET surface area of T300 and T700SC carbon fibres as a function of fluorination time.

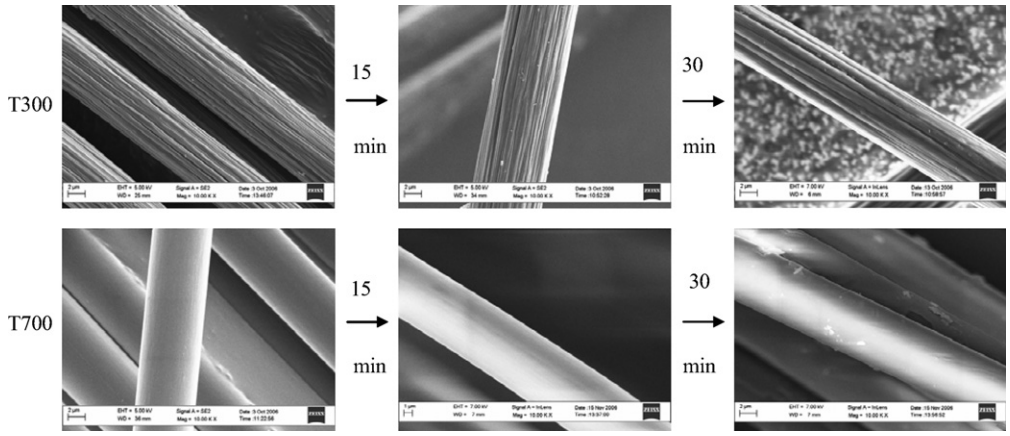

Fig. 3. SEM images of direct fluorinated T300 and T700SC carbon fibres surfaces as fluorination time increases.

The measured ζ-potentials as a function of pH (Fig. 5) of the desized but industrially oxidised T300 and T700 carbon fibres (T3A, T7A) show the typical behaviour of solids containing Brønsted acid groups as indicated by the low isoelectric point (iep), where $\zeta = 0$, and a $\zeta_{plateau}$ in the alkaline region. Even though as a result of direct fluorination where the fibre surface is almost completely fluorinated, $\zeta = f(\text{pH})$ for the T300 fibres does not change at all except for the T300E fibres. The fluorinated carbon fibres still have an acidic surface character. The hydrophobic nature of the fluorinated carbon fibres prohibited them from coming into contact with water and therefore it is expected in this case that ion adsorption dominates the formation of the electrical double layer. Since all fluorinated fibres have the same surface composition, all $\zeta = f(\text{pH})$ are identical, except for the fibres with the highest degree of bulk fluorination, which have a very much higher $\zeta_{plateau}$ which could be due to an overlaid F^- desorption from the bulk of the fibres. In the case of the T700 fibres directly fluorinated in a F_2/N_2 atmosphere, the surfaces appear to have a slightly more acidic character than the industrially oxidised and desized carbon fibres as can be seen by the shift of the iep from pH 3.6 to 3.2. The reason for the minor shift in iep is due to the fact that the fibre surfaces are not completely fluorinated $\zeta = f(\text{pH})$ and still contain a few acidic oxygen surface characteristic functional groups after direct fluorination modification, which now have lower pK_a caused by the introduction of fluorine in the vicinity of the acid groups. The presence of varying amounts of –COOH causes the scatter of

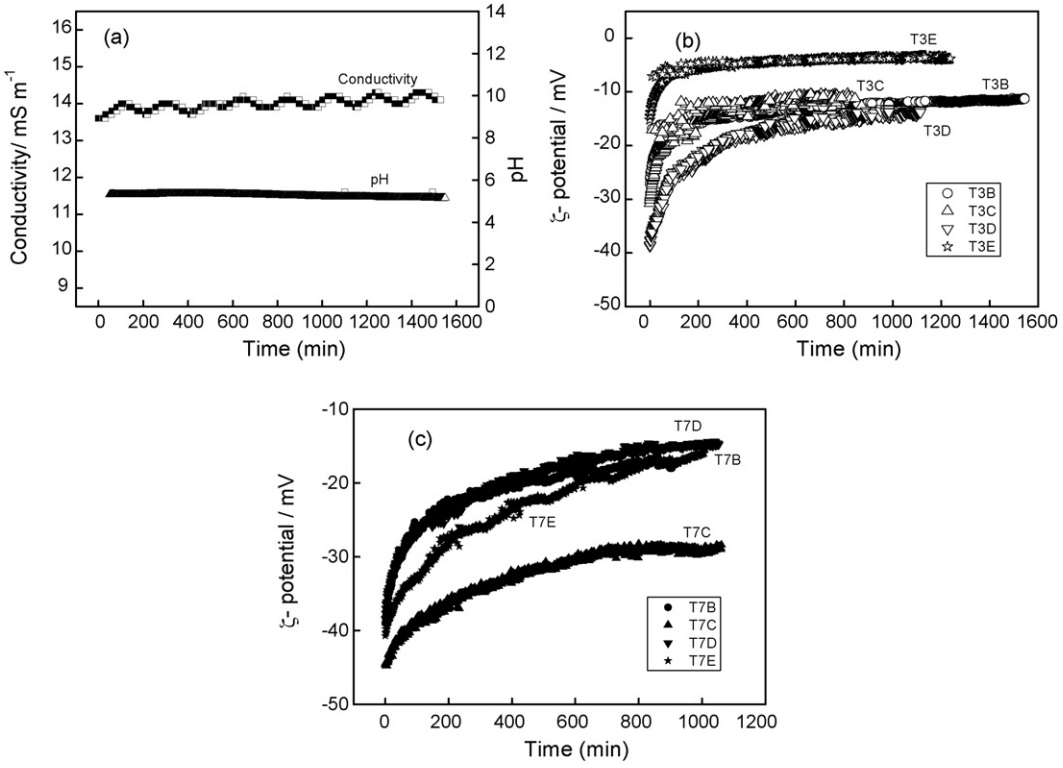

Fig. 4. Time-dependent study of direct fluorinated T300 and T700SC carbon fibres as function of time (a) conductivity and pH (exemplarily), (b and c) ζ-potential.

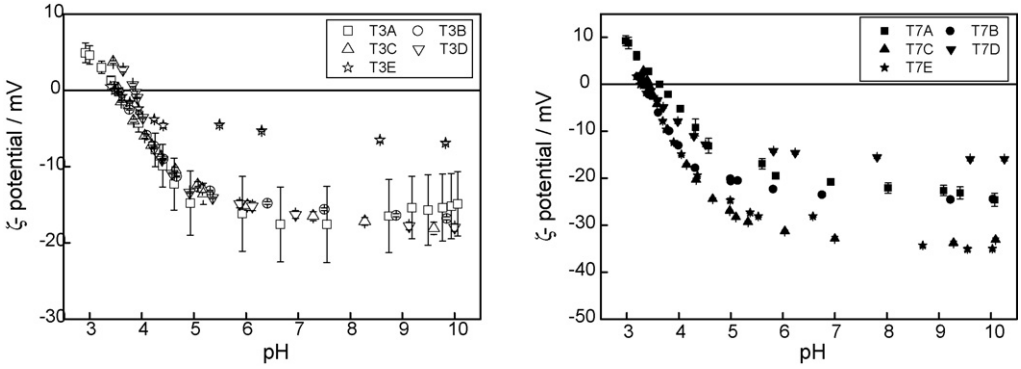

Fig. 5. ζ-Potential as function of pH of direct fluorinated T300 and T700 SC carbon fibres.

the $\zeta_{plateau}$ values, however, the fluorinated T7B and T7D carbon fibres have a very much higher $\zeta_{plateau}$. Also, in these cases the ζ-potential and charge formation seems to be overlaid by the dissociation and desorption of F^- from the "bulk" of the fibres. Both fibres also have a slightly higher electrical conductivity (Table 4) as well as a violet colour appearance compared with the rest (Fig. 1), which is evidence for the formation of fluorine-intercalated carbon fibres.

2.4. Bulk properties of direct fluorinated carbon fibres

2.4.1. X-ray diffraction (XRD)

The XRD patterns of directly fluorinated T300 and T700 carbon fibres with increasing bulk fluorine content are shown in Fig. 6. A broad diffraction line is observed near $2\theta \approx 24^\circ$ for all carbon fibres investigated. In addition, extra broad diffraction lines between $2\theta \approx 10$–15° and 44° were also observed for the highly fluorinated carbon fibres T3D and T3E as well as T7D–T7E. The diffraction line between $2\theta \approx 10$ and 15° corresponds to the 0 0 1 plane and is due to formation of carboneous fluoride in the carbon fibres. The diffraction lines around $2\theta \approx 24^\circ$ and 44° correspond to the 0 0 2 and 1 0 0/1 0 1 lines of the graphitic structure, respectively [30]. Although with increasing fluorination time the 0 0 2 diffraction profile becomes narrower indicating changes in the turbostratic graphite structure of the T300 carbon fibres, in particular for the heavily fluorinated fibres T3D and T3E, no shifts in the peak position can be detected. Although the calculated interlayer distance $d_{0\,0\,2}$ did not change for the T300 fibres, a decrease in the full width at half maximum (β) indicates an increase in crystallite size, or apparent stack size, L_c (0 0 2) which is due to bulk fluorination in the 0 0 2 plane. For the fluorinated T700 carbon fibres a shift of the diffraction line of graphite (2θ) towards a higher angle, which indicates bulk fluorination as well as a narrowing of the 0 0 2 diffraction line, i.e. corresponding to an increase in L_c, was observed (Table 4).

Table 4
Full width at maximum height (FWMH), calculated interlayer distance (d), crystallite size (L_c) and conductivity (κ) of direct fluorinated T300 and T700SC carbon fibres

Fibre	FWMH (°)	$d_{0\,0\,2}$ (Å)	L_c (nm)	κ (S cm^{-1})
T3A	5.7	3.59	0.27	637
T3B	4.9	3.59	0.32	602
T3C	4.9	3.59	0.32	609
T3D	4.2	3.59	0.37	593
T3E	4.2	3.59	0.37	580
T7A	4.2	3.60	0.37	905
T7B	3.9	3.56	0.40	1022
T7C	3.7	3.56	0.42	894
T7D	4.1	3.59	0.38	990
T7E	4.0	3.56	0.39	884

2.4.2. Influence of direct fluorination on the electrical conductivity of the fibres

Electrical conductivity measurements allow detection of changes in the π-electron system of the graphitic parts of the carbon fibres. Such changes in the π-electron system indicate changes in the bulk properties caused by the reaction with fluorine inside the fibres [14]. The results in Table 4 show that the electrical conductivity of direct fluorinated T300 fibres decreased by up to 8%, while direct fluorination only marginally affects the conductivity of the T700 carbon fibres. The increase in electrical conductivity observed for the fluorinated fibres T7B and T7D could be due to intercalation of fluoride species into the carbon fibres [14] but no further evidence for intercalation was found. However, the decrease in fibres electrical conductivity of treated T300 fibres indicates formation of covalent CF bonds which agrees with the results obtained by Tressaud et al. [17,18].

2.4.3. Raman spectroscopy

The spectra, showing the two characteristic peaks at around 1350 and 1580 cm^{-1}, are typical of the high wave number region of graphite materials. These peaks for graphitic sp^2 carbon are associated with disorder finite-sized microcrystalline carbon (D-band) and tangential graphitised carbon (G-band), respectively [31,32]. The ratio between the defective and graphitic band of directly fluorinated carbon fibres was calculated, as it is a measure of dislocations and crystallite modes in carboneous materials. Although from the spectra (Fig. 7) no particular trend and shifts can be seen for the D and G peaks, the calculated integral ratio of the deformation and crystalline mode for the T300 fibres show that the ratio of disordered to pure graphitic regions of the carbon fibres increases steadily with increasing time of direct fluorination. In the case of the T700 fibres, the structural changes appear to be marginal as the number of defective sites only increases after

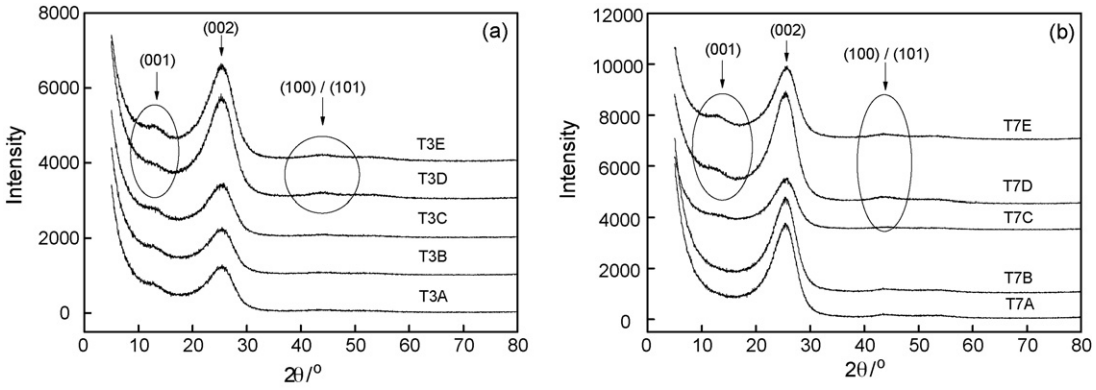

Fig. 6. X-ray diffraction profiles of direct fluorinated carbon fibres (a) T300 fibres and (b) T700SC fibres.

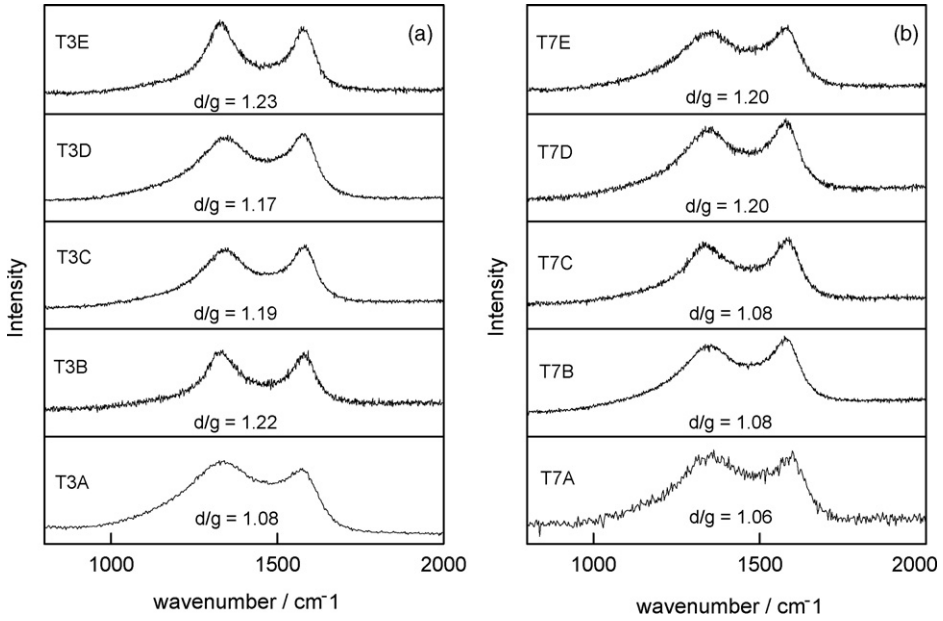

Fig. 7. Raman spectra and ratio of degenerate of deformation mode (d) and crystallite mode (g) of direct fluorinated (a) T300 and (b) T700SC carbon fibres.

25 min of direct fluorination. The SEM images of the fibres (Fig. 3) also show that the T700 fibres are more homogeneous even after fluorination than the T300 fibres, which is consistent with the Raman findings. The T700 fibres seem to be more resistant to fluorination as confirmed by the smaller increase in the crystallite size as derived from the XRD analysis as compared to the T300 fibres (Table 4). From the elemental analysis results (Table 1), a bulk fluorine content of 14.4 mass% was achieved after 30 min of direct fluorination for the T300 carbon fibres, whereas only a bulk fluorine content of 10.4 mass% was achieved after 30 min of direct fluorination for the T700 carbon fibres.

2.4.4. *Influence of direct fluorination to fibres tensile strength*

The impact of direct fluorination on the mechanical properties of the carbon fibres was studied by means of single fibre tensile tests. Fig. 8 shows the tensile strength and Young's modulus of single carbon fibres as a function of the bulk fluorine content. The tensile strength of the fluorinated T300 fibres decreased by 33% and the Young's modulus by 20%, which is largely due to surface damage, formation of pit holes and the bulk fluorination of the carbon fibres [14,20]. For the T700 fibres, given the error, the effect of direct fluorination on the tensile strength and Young's modulus is marginal. The large

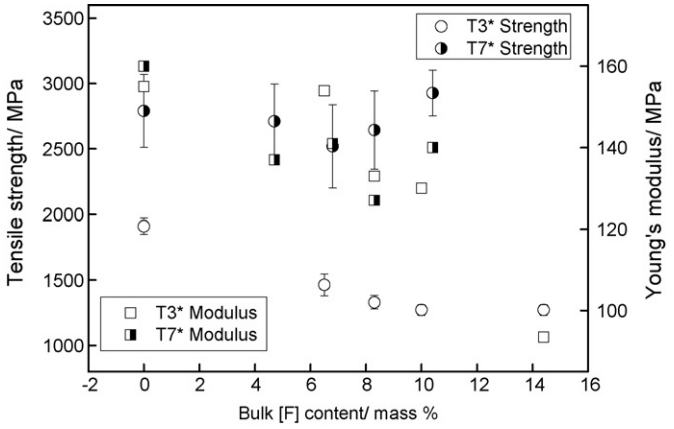

Fig. 8. Variation of tensile strength and Young's modulus as a function of bulk fluorine content bulk fluorine content of T300 and T700SC carbon fibres.

scatter of the tensile strength and the Young's modulus is most likely due to the variable fibre diameter [33] (see also in Table 3). Nonetheless, the drop in the tensile strength of the T300 fibres does not necessarily disqualify the fibres for use in composites, especially if other important physical properties have been significantly improved [14].

3. Conclusion

To achieve the goal of ultra-inert composites, chemically inert and durable fluorinated carbon fibres are required. Carbon fibres were fluorinated in a fluorine/nitrogen atmosphere at a temperature of 653 K. The impact of fluorination on the surface and bulk properties of the carbon fibres was studied. A range of different carbon fibres with increasing bulk fluorine content was synthesised using a blend of fluorine and nitrogen gas. The first indication of severe fluorination was the dramatic change in colour of the fibres. However, the surface fluorine content of the severely fluorinated fibres remained constant at around 64 at.%. The surfaces of the fluorinated carbon fibres contained mainly covalent C–F_x species as shown by XPS and ζ-potential measurements. As a result a dramatic increase in surface hydrophobicity was observed by contact angle measurements as a result of direct fluorination. As expected, the fibre surfaces became PTFE-like, with a surface tension of $\gamma \approx 20$ mN m^{-1}. However, the BET surface area increased drastically after fluorination due to the removal of amorphous carbon from the fibre surfaces. Raman spectra and XRD show that the bulk properties of the fluorinated fibres are only marginally affected, nevertheless the electrical conductivity for most of the fluorinated fibres decreases by up 8%, which may have arisen from the etching of insulating carbon impurities by fluorination. For the T300 carbon fibres the tensile strength decreased by up to 30% which is most likely due to surface damage and the formation of pit holes during fluorination, which also causes the large increase in surface area. The changes in tensile strength and Young's modulus of the T700 fibres appear to be marginal. The T700 fibres appear to be more resistant to fluorination as seen by the smaller increase in crystallite size compared with the T300 fibres. Consequently, direct fluorination has shown maximum alteration to the surface properties of the fibres by the introduction of covalent C–F bonds while interruptions to the bulk properties can be kept to a minimum.

4. Experimental

4.1. Materials

The carbon fibres used in this study were polyacrylonitrile (PAN)-based standard modulus T300 (FT300-6000-99) and high tensile strength T700SC carbon fibres. They were both kindly supplied by Torayca (Toray Industries, Tokyo, Japan). Both carbon fibres were sized to allow easier handling and better compatibility to epoxy matrices. However, during the direct fluorination procedure the sizing was burnt off. Prior to the characterisation of the original industrially oxidised carbon fibres, the sizing was removed by Soxhlet extraction in acetone for 48 h. After Soxhlet extraction the fibres (T3A and T7A) were dried in a vacuum oven for 24 h at 60 °C in order to remove any residual solvent.

4.2. Direct fluorination

Highly fluorinated T300 (T3) and T700 (T7) carbon fibres were obtained by fixing cut carbon fibres (190 mm) onto nickel screens to facilitate a homogeneous gas flow around the fibres. The sample racks were then placed in a nickel reactor held at 653 K and exposed to a blend of 10 vol.% fluorine in nitrogen at a flow rate of 0.2 L min^{-1} at atmospheric pressure for 15 min (T3B, T7B), 20 min (T3C, T7C), 25 min (T3D, T7D) and 30 min (T3E, T7E). The fluorine was produced in the laboratory by electrolysis of a KF/HF melt. The F_2 produced contained 4–5% HF together with small quantity of CF_4 and SF_6 but no metal fluorides in any measurable quantity. **Handling fluorine gas mixtures is hazardous, in order to minimise the potential health and safety hazards we have followed the safety guidelines by Ranken et al.** [34].

4.3. Surface analysis

4.3.1. Appearance and fibre surface morphology

The fluorinated carbon fibres were scanned at 600 dpi using a scanner (Canon, CanoScan Lide 20, Japan) to record the colour of the fluorinated fibres. To investigate the surface morphology of fluorinated carbon fibres, the fibres were fixed on aluminium stubs using carbon tapes and examined using a LEO Gemini FEG-Scanning Electron Microscope (Oberkochen, Germany) without the need for a coating.

4.3.2. Fibre surface chemistry

The surface composition of the fluorinated fibres was determined using X-ray photoelectron spectroscopy. A Scienta ESCA300 photoelectron spectrometer equipped with an Al Kα X-ray source ($h\nu = 1486.7$ eV) was used. The analyser was set to a pass energy of 150 eV for both wide (slit width 1.9 mm) and high resolution scans (slit width 0.8 mm). A thermionic emission electron flood gun was used to achieve charge compensation of the fluorinated carbon fibres. The elemental composition of the fibres was determined using the appropriate sensitivity factors for the elements from the XPS-wide scans and high resolution spectra.

4.3.3. Determination of the fibre diameter and surface wettability

The diameter and surface wettability of the direct fluorinated carbon fibres were determined using the modified Wilhelmy-technique [23]. To determine the wetted perimeter or diameter of the fibres a fully wetting liquid has to be used. Measurements are performed using *n*-dodecane ($\gamma_{lv} = 25.4$ mN m^{-1}, 99% purity, Fisher Scientific, UK). The absence of any contact angle hysteresis during the measurements when using a low surface tension liquid is taken as indicator for complete wetting. The mass changes m during wetting and de-wetting of the fibres were recorded using an ultra-microbalance (4504 MP8,

Sartorius, Göttingen, Germany; accuracy = 0.1 μg) and the fibre diameter d_f was calculated using Eq. (1):

$$d_f = \frac{mg}{\pi \cdot \gamma_{lv}} \quad (1)$$

where g is the acceleration due to gravity and γ_{lv} is the surface tension of *n*-dodecane. Advancing (θ_a) and receding (θ_r) contact angles against different test liquids (deionised water, $\gamma_{lv} = 72.8$ mN m^{-1}; formamide, $\gamma_{lv} = 58.2$ mN m^{-1}; diiodomethane $\gamma_{lv} = 50.8$ mN m^{-1}, 99% purity, Fisher Scientific, UK) were determined by measuring again the mass change m, recorded using the same ultra-microbalance, during immersion and emersion of the fibre into and from the test liquids, using the Wilhelmy equation:

$$\cos\theta = \frac{mg}{\pi \cdot d_f \cdot \gamma_{lv}} \quad (2)$$

For each measurement 5 single fibres were used and at least 25 single fibre samples from each directly fluorinated sample batch were characterised to obtain a statistical significant average of the fibre diameter. The errors are presented as standard deviation.

4.3.4. Determination of the fibre surface tension

The surface tension of the carbon fibres (γ_s) was estimated from measured contact angles using the equation-of-state surface tension model [26]. This requires that the contact angles between the fibres and at least one test liquid with known surface tension must be measured. This approach assumes that the contact angle of a liquid on a solid is solely determined by the solid surface energy and the liquids surface tension. For further details see the following reviews [35–37].

4.3.5. Fibre surface area: BET N_2 adsorption

The BET specific surface area (A_s) of the carbon fibres was measured using a Micromeritics ASAP 2010 analyser with oxygen-free N_2, and the surface area calculated according to ISO 9277 [38].

4.3.6. Fibre surface character: Zeta (ζ)-potential measurements

An Electrokinetic Analyser (EKA, Anton Paar KG, Graz, Austria) based on the streaming potential method was used to determine the electrokinetic or ζ-potential of fluorinated carbon fibres. A batch of carbon fibres (1.5 ± 0.2 g) was placed into a glass cylindrical cell where it was tightly packed between two perforated PMMA caps and sandwiched between two perforated Ag/AgCl electrodes. The system was filled and rinsed with 1 mM KCl electrolyte solution. All entrapped air bubbles in the fibres were removed at this stage. A pressure drop across the sample starting at 30 mbar which steadily increases to 150 mbar was generated while the electrolyte was pumped through the cylindrical cell. To ensure that the fluorinated carbon fibres are stable with time, the ζ-potential was measured over a period of time at constant temperature (20 °C) in 1 mM KCl. The pH-dependence of the ζ-potential was measured starting from neutral pH down pH 3 and up to pH 10, respectively. The pH change was achieved by adding 0.1 M HCl or 0.1 M KOH by means of an auto titrating unit (RTU, Anton Paar KG, Graz, Austria).

4.4. Bulk analyses of direct fluorinated carbon fibres

4.4.1. Carbon fibre bulk composition

The bulk fluorine content of treated carbon fibres was determined using elemental analysis. Fibre samples were carefully decomposed in sodium peroxide. The liberated fluoride was determined by titration with thorium nitrate [10]. The bulk fluorine content can be determined with an accuracy of ±1 mass%.

4.4.2. X-ray diffraction (XRD) analysis

A small aligned fibre batch was clamped flat onto a single crystal silicon wafer and aligned perpendicular to the incident X-ray beam. XRD analysis was undertaken using a Philips PW1700 series automated powder diffractometer operated at 40 kV and 40 mA with a secondary graphite crystal monochromator and Cu Kα source, scanning between 5° and 80° in 0.04° steps. The crystallite size (L_c), which reflects on the structural order, was determined using the Scherrer equation:

$$L_c = \frac{K\lambda_L}{\beta \cdot \cos\theta} \quad (3)$$

where β is the full width at half maximum of the diffraction peak, $K = 0.91$ a constant, λ_L the X-ray wavelength and θ is the scattering angle.

4.4.3. Raman spectroscopy

Raman spectra were acquired using a LabRam Infinity Analytical Raman Spectrometer (Jobin Yvon Horiba, Middlesex, UK) equipped with a green 532 nm laser. The spot size was reduced to a minimum while the laser power was at 100% strength. At least six spectra were recorded at different spots of the same sample and averaged. The aperture was set to 200 μm with an acquisition time of 10 s and a grating of 1800 grooves mm^{-1}. The measurements were carried out at room temperature while scanning a range from 800 to 2000 cm^{-1}. The experimental results of Raman spectra were peak fitted using a mixed Gaussian–Lorentzian curve in order to determine the peak intensities and Raman shifts.

4.4.4. Electrical conductivity of fluorinated fibres

The four-point method was used to determine the electrical conductivity of single carbon fibres, which allows eliminating problems of contact resistance [39]. A constant voltage of 10 V, supplied by a DC Voltage Calibrator (0.02% grade, Time Electronics Limited, Kent, UK) was amplified (by a Krohn-Hite Model 7500 amplifier, Brockton, USA) and passed through the carbon fibre. The current across the two-point sector was then recorded by a digital multimeter (Keithley 195A, Cleveland, OH, USA) and the resistance (R) was calculated. The resistivity (ρ) of a single filament was calculated using the fibre length ($l = 2$ cm) and the measured fibre diameter ($d_f \approx 7$ μm, see

Table 3 for the exact values) using the following equation:

$$\rho = \frac{R \cdot \pi \cdot d^2}{4l} = \frac{U \cdot \pi \cdot d^2}{I \cdot 4l} = \frac{1}{\kappa} \quad (4)$$

where κ is the specific conductivity, U the applied voltage and I is the measured current. All measurements were repeated at least on 10 different samples of each type to obtain a statistical average. The errors are presented as standard deviation.

4.4.5. Influence of direct fluorination on fibres tensile strength

The effect of fluorination on the tensile strength of carbon fibres was determined using a tensiometer (Biax 200L, Micro Materials Ltd., Wrexham, UK) following the ISO British Standard [40]. For each measurement a single carbon fibre was glued onto a paper frame using cyanoacrylate adhesive. The gauge length, i.e. free fibre length, was set to 25 mm. The single fibre was loaded at a rate of 0.01 mm s^{-1} until the fibre failed while the loading force versus displacement were logged using a computer. For each fibre, the tensile strength and Young's modulus are calculated using Eqs. (5) and (6):

$$\sigma_f = \frac{F}{A_f} \quad (5)$$

$$E = \frac{F/A_f}{\Delta L/L_0} \quad (6)$$

where σ is the tensile strength (MPa), F the tensile force (N) at break and A_f the fibre cross-sectional area (mm^2); E the Young's modulus (MPa), L_0 the original length of the fibre and ΔL is the change in length of the fibre when subjected to an applied force. All measurements were repeated at least on twenty different samples of each type to obtain a statistical average. The errors are presented as standard errors.

Acknowledgements

Our research was made possible by the financial support of the UK Engineering and Physical Science Research Council (EPSRC) (Grant Award No.: GR/S75673/01). We would like to thank Vladimir Arye for arranging and assisting with shipping and fluorinating the fibre samples (Lodester, Inc., Howell, NJ, USA). We thank Michael Q. Tran (*PaCE*, Imperial College London) for taking the SEM images. We also acknowledge the support of the STFC (Daresbury Laboratory, Warrington, UK) for enabling the XPS characterisation of the fluorinated carbon fibres.

Appendix A. Supplementary data

Supplementary data associated with this article can be found, in the online version, at doi:10.1016/j.jfluchem.2007.06.005.

References

[1] F.N. Cogswell, Thermoplastic Aromatic Polymer Composites, Butterworth-Heinemann, Oxford, 1992, pp. 34–39.
[2] A. Shindo, in: S.L. Phoenix, I.J. Beyerlein (Eds.), Polyacrylonitrile (PAN)-Based Carbon Fibers, Comprehensive Composite Materials, vol. 1, Elsevier Science, Amsterdam, 2000, pp. 1–33.
[3] L.M. Manocha, Encyclopaedia of Materials: Science and Technology, Elsevier Science, Amsterdam, 2001, pp. 906–916 (Part 1).
[4] J.G. Drobny, Macromol. Symp. 170 (2001) 149–156.
[5] J.G. Drobny, Technology of Fluoropolymers, CRC Press, Boca Raton, 2001.
[6] S.S. Wang, High Performance Composites, March 2006.
[7] N.L. Ulstein, B. Nygreen, J.R. Sagli, Euro. J. Oper. Res. 176 (2007) 550–564.
[8] H. Selig, M. Zayat, D. Davidov, J. Fluorine Chem. 54 (1991) 130.
[9] A. Bismarck, E. Schulz, J. Mater. Sci. 38 (2003) 4965–4972.
[10] K.K.C. Ho, G. Kalinka, M.Q. Tran, N.V. Polyakova, A. Bismarck, Comp. Sci. Technol. 67 (2007) 2699–2706.
[11] K.K.C. Ho, S. Lamoriniere, G. Kalinka, E. Schulz, A. Bismarck, J. Colloid Interface Sci. 313 (2007) 476–484.
[12] A. Bismarck, R. Tahhan, J. Springer, A. Schulz, T.M. Klapötke, H. Zell, W. Michaeli, J. Fluorine Chem. 84 (1997) 127–134.
[13] Y. Chong, H.J. Ohara, J. Fluorine Chem. 57 (1992) 169–175.
[14] M. Zayat, D. Davidov, H. Selig, Carbon 32 (1994) 485–491.
[15] K.K.C. Ho, A.F. Lee, A. Bismarck, Carbon 45 (2007) 775–784.
[16] V. Gupta, R.B. Mathur, O.P. Bahl, A. Tressaud, S. Flandrois, Synth. Met. 73 (1995) 69–75.
[17] A. Tressaud, V. Gupta, L. Piraux, L. Lozano, E. Marquestaut, S. Flandrois, A. Marchand, O.P. Bahl, Carbon 32 (1994) 1485–1492.
[18] A. Tressaud, C. Guimon, V. Gupta, F. Moguet, Mater. Sci. Eng. B 30 (1995) 61–68.
[19] H. Touhara, F. Okino, Carbon 38 (2000) 241–267.
[20] N. Watanabe, T. Nakajima, H. Touhara, Graphite Fluoride, Studies in Inorganic Chemistry, Elsevier, Amsterdam, 1988, pp. 71–87 (Chapter 8).
[21] L. Fischer, U. Siemann, W. Ruland, Colloid Polym. Sci. 261 (1983) 744–749.
[22] R. Holm, S. Storp, Ullmanns Encyclopädie der Techischen Chemie, vol. 5, Verlag Chemie GmbH, Weinheim, 1980, pp. 519–576.
[23] G.E. Collins, J. Textile Inst. 38 (1947) T73–T77.
[24] R.E. Johnson Jr., R.H. Dettre, Contact Angle Wettability and Adhesion, Advances in Chemistry Series 43, American Chemical Society, Washington, D.C., 1964, pp. 112–135.
[25] R.H. Dettre, R.E. Johnson Jr., Contact Angle Wettability and Adhesion, Advances in Chemistry Series 43, American Chemical Society, Washington, D.C., 1964, pp. 136–144.
[26] C.A. Ward, A.W. Neumann, J. Colloid Interf. Sci. 49 (1974) 286.
[27] S.R. Coulson, I.S. Woodward, J.P.S. Badyal, Langmuir 16 (2000) 6287–6293.
[28] P. Morgan, Carbon Fibres and their Composites, vol. 9, CRC Press, NY, 2005, pp. 347–350.
[29] A. Bismarck, J. Springer, Colloids Surf. A 159 (1999) 331–339.
[30] V.S. Babu, M.S. Seehra, Carbon 34 (1996) 1259–1265.
[31] G.A. Zickler, B. Smarsly, N. Gierlinger, H. Peterlik, O. Paris, Carbon 44 (2006) 3239–3246.
[32] N. Meyer, G. Marx, K.W. Brzezinka, Fresenius J. Anal. Chem. 349 (1994) 167–168.
[33] T. Tagawa, T. Miyata, Mater. Sci. Eng. A 238 (1997) 336–342.
[34] E.A. Ranken, C.V. Borzileri, The Safe Handing of Fluorine, Health and Safety Manual, Supplement 21.12, University of California, Lawrence Livermore National Laboratory, Berkeley, 1987.
[35] D.Y. Kwok, A.W. Neumann, Colloids Surf. A 161 (2000) 31–48.
[36] D.Y. Kwok, A.W. Neumann, Colloids Surf. A 161 (2000) 49–62.
[37] S. Cantin, M. Bouteau, F. Benhabib, F. Parrot, Colloids Surf. A 276 (2006) 107–115.
[38] ISO, ISO9227, Determination of the Specific Surface are of Solids by Gas Adsorption Using the BET Method, International Organization for Standardisation, 1995.
[39] DIN, 53 482, Method of Test for Materials for Electrical Purposes, Measuring of Electrical Resistance of Non-metallic Materials.
[40] BS ISO, 11566:1996, Carbon Fibre—Determination of the Tensile Properties of Single-Filament Specimens.